MONITORING ATMOSPHERIC DUST OPACITY AT HIGH LATITUDES ON MARS BY IMAGING SPECTROSCOPY.

S. Douté[1], **X. Ceamanos**[1], **T. Appéré**[1], [1]*Institut de Planétologie et d'Astrophysique de Grenoble (IPAG), France*, **M. Vincendon**[2], **Y. Langevin**[2], **and the OMEGA Team,** [2]*Institut d'Astrophysique Spatiale (IAS), Orsay, France*, **(sylvain.doute@obs.ujf-grenoble.fr).**

Introduction

Micrometer sized mineral particles drifting over Mars surface greatly influence both solar and thermal radiative fluxes in the atmosphere, thus its energy balance and its global circulation. Furthermore any kind of remotely sensed data in the optical domain includes their strong, spatially varying, often annoying contributions. Monitoring the particles as well as identifying the sources and the sinks in relation with surface activity is of paramount importance especially at high southern latitudes in spring. Since 2004 the imaging spectrometer OMEGA on board Mars Express performs nadir-looking and EPF observations in the VIS and the NIR for the study of the surface and atmosphere alike.

The authors in [1] have developed a method to quantify the contribution of atmospheric dust in near-IR spectra obtained by the OMEGA regardless of the Martian surface composition. Using observations in the nadir pointing mode with significant differences in solar incidence angles, they can infer the optical depth of atmospheric dust, and retrieve the surface reflectance spectra free of aerosol contribution. However this method relies on the very restrictive assumption that the atmosphere opacity remains approximately constant during the time spanned by all the employed acquisitions.

In [2] the same authors have mapped the total optical depth of dust aerosols in the near-IR above the south seasonal cap of Mars from mid-spring to early summer. This mapping is based on the assumption that the reflectance in the 2.64 μm saturated absorption band of the surface CO_2 ice is mainly due to the light scattered by aerosols above most places of the seasonal cap. In this case one geometry is sufficient for the retrieval but it is restricted to the area of CO_2 deposits not contaminated by dust and water.

We aim at proposing an original method that overcomes these limitations to retrieve the optical depth of the Martian dust at a reference wavelength of one micron. The method is based on a parametrization of the radiative coupling between particles and gas that determines, with local altimetry and the meteorological situation, the absorption band depth of gaseous CO_2. We are complementary to the method of [2] since our approach specifically treats pixels occupied by purely mineral surfaces or icy deposits contaminated by a large amount of dust while being observed at a fixed geometry. After validation, we apply both methods in order to map atmospheric dust opacity at high southern latitudes from early to late spring of Martian Year 27. For that purpose we use a time series of OMEGA images for global coverage. In section 1, we give insights about Martian atmospheric properties and radiative transfer in the near infrared range. We describe models that calculate the spectral radiance coming from Mars and reaching the sensor at the top of the atmosphere. In section 2 we explain how we implement these models for retrieving the aerosol optical depth from the images. In section 3 we present and interpret the maps of atmospheric opacity and surface Lambert albedo resulting from the analysis of the selected series of OMEGA images.

1 Mars atmospheric radiative transfer

Gas A dozen atmospheric absorption bands due to gaseous CO_2 and marginally to H_2O are present on the near infrared spectra. We calculate the transmission function of the atmosphere along the vertical, for each pixel of our spectral images, and as a function of wavelength. For that purpose, we employ a line-by-line radiative transfer model (LBLRTM) [3] fed by the vertical compositional and thermal profiles predicted by the European Mars Climate Database (EMCD) [4] for the dates, locations, and altitudes of the observations.

We divide the Martian atmosphere into 35 plan-parallel layers spanning the 0-100 km height range. LBLRTM gives for each layer l and for each channel k of the instrument a spectrum of optical depth at very high spectral resolution (10^{-4} cm^{-1}) from which we calculate the inverse of the cumulative frequency distribution $\tau_{gaz}(g), g \in [0,1]$. As in [5] we then calculate the mean optical depth $\bar{\tau}^{l,k}_{gaz\ i}$ over 16 specified subintervals Δg_i that follow the Gaussian quadrature (g_i, a_i). Assuming the τ_{gaz} distributions are correlated between layers, the transmission function through the atmospheric gases along the vertical can be approximated by :

$$T^k_{gaz} = \sum_i^{16} a_i \exp(-\sum_l \bar{\tau}^{l,k}_{gaz\ i})$$

Because the complete calculation is very time consuming, it is only performed for a limited ($\lesssim 20$) number of reference points representative of "regions" sliced according to regular bins in latitude lat, longitude $long$

and altitude h. Three transmission spectra are generated for the maximum, mean and minimum altitude of a given region. Then the transmission spectrum of all the pixels belonging to the region is interpolated from the triplet depending on their individual altitude to give $T^k_{gaz}(h, lat, long)$

Aerosols Optical properties of Martian mineral aerosols are still largely undocumented even though recent studies have improved our understanding [6]. We favor the single scattering albedo, optical depth shape and phase function retrieved in the IR by [2]. We take an exponentially decreasing number density of aerosol particles such that the vertical distribution of optical depth at a reference wavelength (k_0 : 1 μm) is given by :

$$\begin{aligned}\tau^{l,k_0}_{aer} &= \tau^{k_0}_{aer}(\exp(-z^l/H_{scale}) - exp(-z^{l+1}/H_{scale})) \\ &\quad /(1-\exp(-zmax/H_{scale}))\end{aligned}$$

$\tau^{k_0}_{aero}$ is the column integrated opacity of the aerosols, H_{scale} is the scale height of the distribution, z^l the height of layer l lower interface and $zmax = 100$ km.

Top of the atmosphere radiance We consider the atmosphere as a plan parallel vertically stratified medium which is a good approximation to calculate the top of the atmosphere (TOA) radiance whenever incidence and emergence directions are $\approx 10°$ above the horizon. The surface is characterized by its bidirectional reflectance distribution function (BRDF). In general photons undergo absorption and multiple scattering events when interacting both with gas and aerosols. As a consequence calculating at channel k the transfer of radiation in the atmosphere requires to couple gas and aerosols properties at each atmospheric level l and for each quadrature g_i. Such operation leads to the optical depth, single scattering albedo and phase function of the layers that are introduced in the DISORT algorithm along with the acquisition geometry (θ_0, θ, ϕ) to calculate the TOA partial radiance $I^k_i(\theta_0, \theta, \phi)$. The total radiance is given by :

$$I^k(\theta_0, \theta, \phi) = \sum_i^{16} I^k_i(\theta_0, \theta, \phi)$$

2 Method for retrieving the optical depth

The method is based on a parametrization of the radiative coupling between particles and gas that determines, with local altimetry and the meteorological situation, the absorption band depth of gaseous CO_2. The coupling depends on (i) the acquisition geometry (ii) the type, abundance and vertical distribution of particles (iii) the surface albedo A^k_{surf}. For each spectro-pixel of an image, we compare the depth of the 2 μm absorption band of gaseous CO_2 that we estimate on the one hand from the observed spectrum and on the other hand from a calculated transmission spectrum through the atmospheric gases alone. This leads to a precious new observable that directly depends on τ^{k0}_{aer}. Combining the latter with the radiance factor $R^{k_1}_{obs}$ deep into the 2 μm band, we evaluate by radiative transfer inversion τ^{k0}_{aer} and A^k_{surf}.

Hypothesis We parametrize the radiative coupling between aerosols and gas by assuming that the latter contribute to the signal as a simple multiplicative filter :

$$\begin{aligned}I^k(\theta_0, \theta, \phi) &\approx T^k_{gaz}(h, lat, long)^{\epsilon(\theta_0, \theta, \phi, \tau^{k0}_{aer}, H_{scale}, A^k_{surf})} \\ &\quad I^k_{surf+aer}(\theta_0, \theta, \phi)\end{aligned}$$

the effect of the acquisition geometry, the aerosols, and the surface Lambertian albedo A^k_{surf} being taken into account by scaling the aerosol free vertical transmission $T^k_{gaz}(h, lat, long)$ - calculated according to 1 - by an exponent ϵ.
$I^k_{surf+aer}(\theta_0, \theta, \phi)$ is the calculated TOA radiance but without considering the atmospheric gases in the radiative transfer. Factor ϵ can be further decomposed into two terms :

$$\begin{aligned}\epsilon(\theta_0, \theta, \phi, \tau^{k0}_{aer}, H_{scale}, A^k_{surf}) &= \psi(\nu). \\ &\quad \beta(\theta_0, \theta, \phi, \tau^{k0}_{aer}, H_{scale}, A^k_{surf})\end{aligned}$$

with the airmass $\nu = \frac{1}{\cos(\theta_o)} + \frac{1}{\cos(\theta)}$. Factor ψ allows a quick and simplified calculation of the free gaseous transmission along the acquisition pathlength using the vertical transmission :

$$\begin{aligned}T'^k_{gaz} &= \sum_i^{16} a_i \exp(-\sum_l \bar{\tau}^{l,k}_{gaz\ i}.\nu) \\ &\approx (T^k_{gaz})^{\psi(\nu)}\end{aligned}$$

Factor β on the other hand expresses the aerosol effect on gaseous absorption. If (i) β can be estimated experimentally for a given OMEGA pixel and (ii) if one assumes a value for A^{k1}_{surf} then (τ^{k0}_{aer}) can be derived. Indeed function $\beta(\theta_0, \theta, \phi, \tau^{k0}_{aer}, H_{scale}, A^{k1}_{surf})$ is invertible provided that the scale height H_{scale} of the aerosols is known. Several studies such as [2] suggest that $H_{scale} = 11$ km is a good guess.

The factor β can be readily estimated for every OMEGA spectrum that does not show any H_2O or CO_2 ice signature superimposed on the 2 μm CO_2 gas absorption band. A formula similar to the one used in the volcano scan technique [7] is used replacing the Olympus reference transmission spectrum by $(T^k_{gaz})^{\psi(\nu)}$. A specific procedure is necessary for any spectrum marked by the signature of water ice with the possible presence of dust but without spectral contamination by CO_2 ice. A numerical optimization is performed regarding a cost function that depends on β and that expresses the quality of the gaseous absorption correction on the spectra. The quality criteria we choose is the band shape of solid H_2O at 2 μm that must show a unique local minimum

and a simple curvature. Mathematically this criteria is equivalent to the second derivative of the spectrum that must be close to 0 for channels $[k'_1, k''_1]$ covering the H_2O band and sligthly beyond.

Numerical aspects Our optical depth retrieval system uses a multidimensional look-up table (LUT) of β values arranged according to discrete combinations of acquisition geometries (θ_0, θ, ϕ) and of physical parameters $(\tau^{k0}_{aer}, H_{scale}, A^{k1}_{surf})$. The values were calculated from synthetic TOA spectra generated by DISORT (I^k and $I^k_{surf+aer}$) :

$$\beta(\theta_0, \theta, \phi, \tau^{k0}_{aer}, H_{scale}, A^{k1}_{surf}) = \sum_{k=k'_1}^{k''_1} f_k \ln(\frac{I^k}{I^k_{surf+aer}}) / \ln(T'^k_{gaz})$$

with $f_k = 1/K$. The channels $k = k'_1, \ldots, k''_1$ ($K = k''_1 - k'_1 + 1$) encompass the 2 μm CO_2 gas absorption band.

For each pixel of an observation the inversion is iterative and starts with two observables $\hat{\beta}$ and $R^{k_1}_{obs}$ and one initial guess for the surface Lambert albedo A^{k1}_{surf}. The LUT is adapted to the desired geometry by multidimensional interpolation and is used to derive τ^{k0}_{aer} from $(\hat{\beta}, A^{k1}_{surf})$. Then a new value of A^{k1}_{surf} is evaluated from $(\tau^{k0}_{aer}, R^{k_1}_{obs}, \hat{\beta})$ until convergence is reached leading to a final value of τ^{k0}_{aer} and to a surface reflectance spectra free of aerosol contribution A^k_{surf}.

Validation Our validation procedure is two-fold. First we build experimentally for several test images curves related $\hat{\beta}$ and ν to be compared to the model $\beta(\nu, \tau^{k0}_{aer}, H_{scale}, A^k_{surf})$. For that purpose we select mineral pixels of a given image approximately at the same altitude but observed at very different geometries. Thus we can assume that the same atmospheric opacity is probed at varied airmass values. In all cases the experimental and observed curves agree very satisfactorily if one chooses the adequate value for τ^{k0}_{aer}. Second a quick cross validation of the two methods we operate consists in ploting transects τ^{k0}_{aer} over adjacent but separated mineral and pure CO_2 regions to check the continuity of values. Unfortunately these regions are often separated by a narrow band of indetermination where none of the method works. Despite of the small gap, examination by eye show that the continuity is good in most cases.

3 Results

The OMEGA instrument has acquired the most comprehensive set of observations to date in the near-infrared (0.93-5.1 microns) on the south seasonal polar cap from mid-winter solstice (L_S=110° , December 2004) to the end of the recession (L_S=320° ,November 2005). See [8] for a complete description. We systematically processed a subset of these observations from L_S=220° to 262° by following the different operations of section 2. As a result, we obtained a series of τ^{k0}_{aer} maps that were de-trended in order to correct for changes due solely to varying atmospheric height because of topography. These maps were independently integrated on a common grid generated from the Hierarchical Equal Area isoLatitude Pixelization (http://healpix.jpl.nasa.gov) of Mars southern hemisphere at different spatial resolutions. Such an integration, possibly followed by averaging over time or latitude bins, makes it easy to create mosaics or to build space-time evolution curves like the ones displayed respectively in Fig.2 and 1.

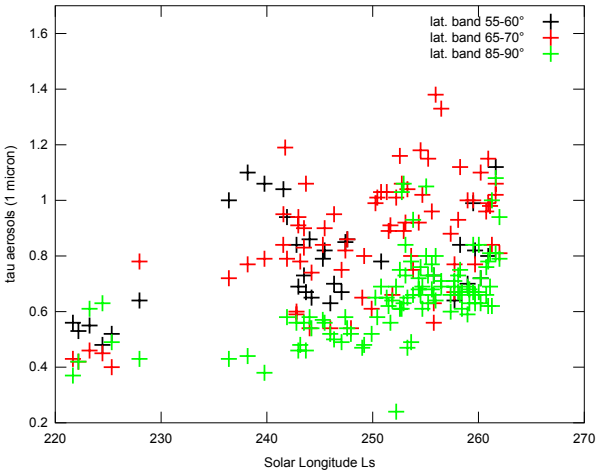

Figure 1: Time evolution of the atmospheric opacity at 1 micron for three different bands of latitude

The atmospheric opacity situation at 1 μm is roughly axisymmetric around the south pole for the period covered by our selection of observations: statistically no significative difference of τ^{k0}_{aer} level according to time is observed between four equal sectors of longitude between 65 and 75° latitude. Consequently we computed the time evolution of the average opacity for a series of latitude bands, Fig.1 showing the three most significant. At the center of the polar seasonal cap, after a period of stagnation at ≈ 0.4 from L_S=220 to 240°, we note a gradual increase of aerosol opacity by a factor of ≈ 2 until the end of the period. The crocus line crosses the latitudinal band 65-70° at $\approx$ 225-235°. Before this event, τ^{k0}_{aer} is comparable to the level of the very high latitudes whereas after L_S 240° it increases rapidly and becomes erratic with much variability, i.e. $\Delta\tau^{k0}_{aer} \approx 0.7$. The latitudinal band 55-60° is already defrosted at the beginning of the period of interest. Then its atmospheric opacity is also comparable to the level of the very high latitudes, but increases sharply to reach a maximum at L_S 240°. Then it drops to return to values typical of the cap which can be considered as a background level.

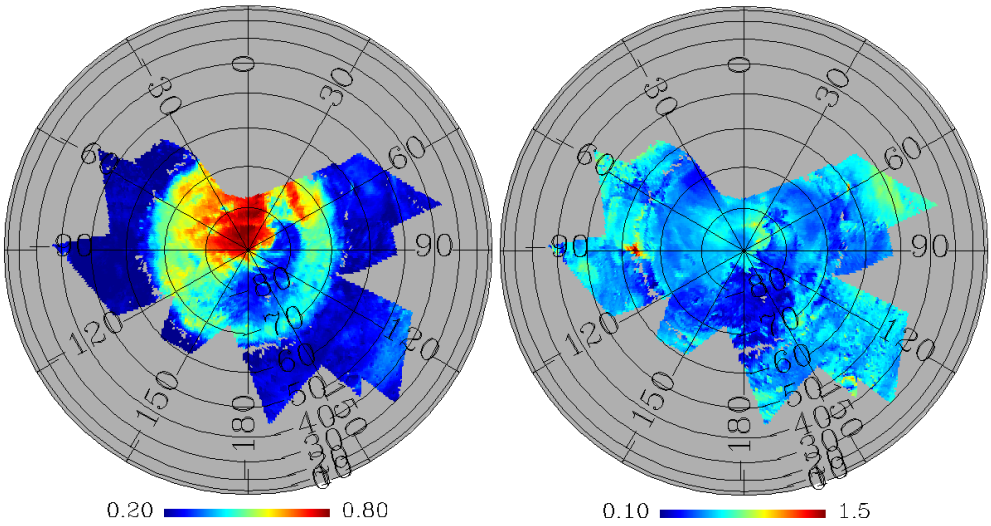

Figure 2: Mosaics built from aerosol optical depth and surface Lambert albedo maps for the L_S range 220-230

At higher spatial resolution the mosaics, such as the one displayed in Fig.2, clearly show the details of dust activity within and around the area covered by the CO_2 seasonal deposits. Around the seasonal cap we note an intense activity, high temporal variability, and a heterogeneous spatial distribution of atmospheric dust with localized enhancement of the optical depth (values up to 1.5). The enhancement takes regional proportions for three different time intervals: 230-240°, 252-254° and 260-262°. Within the seasonal cap, we note lower values than at the outskirts, a more homogeneous spatial distribution and a lower temporal variability even if occasional incursions of dusty clouds from outside the cap can occur.

Conclusions

We propose a method to retrieve the optical depth of aerosols from their strong effect on the intensity of the CO_2 gas absorption bands at high airmass. Experiments conducted on OMEGA nadir looking observations -as well as CRISM EPF [9] - produce good results. Our method works even if the underlying surface is completely made of minerals -low contrast between surface and atmospheric dust- while being observed at a fixed geometry. Nevertheless it provides the maximum of information when applied to spectra acquired over the same area at different emergence angles. The method was applied to a series of OMEGA observations acquired at high southern latitudes from early to late spring of MY 27. Global as well as local investigations about atmospheric dust in relation with surface activity are made possible.

References

[1] M. Vincendon, Y. Langevin, F. Poulet, J.-P. Bibring, and B. Gondet. Recovery of surface reflectance spectra and evaluation of the optical depth of aerosols in the near-IR using a Monte Carlo approach: Application to the OMEGA observations of high-latitude regions of Mars. *Journal of Geophysical Research (Planets)*, 112(E11):8–+, July 2007. doi: 10.1029/2006JE002845. [2] M. Vincendon, Y. Langevin, F. Poulet, J.-P. Bibring, B. Gondet, D. Jouglet, and OMEGA Team. Dust aerosols above the south polar cap of Mars as seen by OMEGA. *Icarus*, 196:488–505, August 2008. doi: 10.1016/j.icarus.2007.11.034. [3] Clough, S. A., Iacono, and M. J. Line-by-line calculation of atmospheric fluxes and cooling rates 2. Application to carbon dioxide, ozone, methane, nitrous oxide and the halocarbons. *J. Geophys. Res.*, 100(9):16519–16536, 1995. [4] F. Forget, E. Millour, S. Lebonnois, L. Montabone, K. Dassas, S. R. Lewis, P. L. Read, M. A. López-Valverde, F. González-Galindo, F. Montmessin, F. Lefèvre, M.-C. Desjean, and J.-P. Huot. The new Mars climate database. In *Mars Atmosphere Modelling and Observations*, pages 128–+, February 2006. [5] A. A. Lacis and V. Oinas. A description of the correlated-k distribution method for modelling nongray gaseous absorption, thermal emission, and multiple scattering in vertically inhomogeneous atmospheres. *J. Geophys. Res.*, 96:9027–9064, May 1991. doi: 10.1029/90JD01945. [6] O. Korablev, V.I. Moroz, E.V. Petrova, and A.V. Rodin. Optical properties of dust and the opacity of the martian atmosphere. *Advances in Space Research*, 35(1):21–30, 2005. [7] P. C. McGuire and 14 co-authors. An improvement to the volcano-scan algorithm for atmospheric correction of CRISM and OMEGA spectral data. *Planetary and Space Science*, 57:809–815, June 2009. doi: 10.1016/j.pss.2009.03.007. [8] Y. Langevin, J.-P. Bibring, F. Montmessin, F. Forget, M. Vincendon, S. Douté, F. Poulet, and B. Gondet. Observations of the south seasonal cap of mars during recession in 2004-2006 by the omega visible/near-infrared imaging spectrometer on board mars express. *J. Geophys. Res.*, 112:–, July 2007. URL `http://dx.doi.org/10.1029/2006JE002841`. [9] Doute, S., Ceamanos, and X. Retrieving mars aerosol optical depth from crism/mro imagery. In *Hyperspectral Image and Signal Processing: Evolution in Remote Sensing, 2010. WHISPERS '10*, pages 1 –4. IEEE, Jun. 2010.